Chapter

Surface Plasmon Resonance Sensors for Concentration and Reaction Kinetic Detections

Xiaoying Wang, Mingqiang Ma, Xueliang Wang and Shoujuan Wang

Abstract

Surface plasmon resonance (SPR) is an optical phenomenon that occurs on the metal (normally gold or silver) film surface and the light that excited this phenomenon changes with the refractive index of materials on the metal surface. SPR sensors are constructed based on this phenomenon and are used in fields of biological and chemical analyses, drug screening, environmental monitoring, and so on. Here, we will make an introduction to applications of SPR sensors on reaction kinetic and concentration detections. To make this chapter readily comprehensible, we will divide it into three portions. The first part will be an abbreviated depiction of surface plasmon excitation and constructions of an SPR sensor. Then, we will aim at an introduction to the bimolecular interactions in SPR sensors. At last, we will make a summary on applications of SPR sensors.

Keywords: surface plasmon resonance, concentration, dissociation constant, kinetics, molecular reaction, sensors

1. Introduction

Surface plasmon phenomenon has been observed for over one century [1], and its applications in sensors have over 40 years [2, 3]. Surface plasmon resonance (SPR) sensors constructed based on this phenomenon are sensitive to the binding and unbinding of molecules on the sensor chip surface [4]. By online recording the reaction process, we obtained the SPR sensorgram and applied it to analyte concentration, especially molecular reaction kinetics analyses. These sensors are applied to the detections of the reactions between protein and protein, protein and DNA/RNA, small molecules and proteins/DNA/RNA, proteins/DNA/RNA/ small molecules and cells, and so on [5–8]. The application fields include chemical and biological analyses, food safety and environmental monitoring, and drug screening [9, 10].

Since the automatic sampling system and a series of commercial chips have been developed, the SPR instruments have been becoming operation-oriented design. And this is further expanding the application fields. But it still cannot maintain the molecular reactions occur at an ideal condition. As the reactions are occurred in solutions, the hydrodynamic conditions are a great variable factor [11]. To be better understanding of this technique and obtaining reliable data, we have to possess a good knowledge on the theory of molecular reactions in the SPR system.

2. SPR sensors

2.1 Excitations of surface plasmon

Surface plasmon (SP) phenomenon was first observed as anomalies in the metallic diffraction grating experiment by wood in 1902 [1]. In 1941, Fano concluded these anomalies on the metallic surface to the excitation of electromagnetic wave [12].

Figure 1 shows the relationship between the incident light angle and the reflected light intensity in the absence and presence of thin gold film [13]. The total reflection occurs at 39 degree in the prism and air system (**Figure 1A** and **B**) and a dip (the drop of reflection) is observed around 43 degree in the presence of gold film (**Figure 1C** and **D**).

This approximated semicircular prism (**Figure 1A** and **C**) makes it possible that the angle of incident light remains unchanged. This significantly simplifies the optical system. As a result, Kretschmann geometry [14], which couples a prism and attenuates the total reflection, is the most common used excitation approach. In another geometry, Otto also used a prism to implement the SP excitation [15], but placed the dielectric layer between the prism and metal layer.

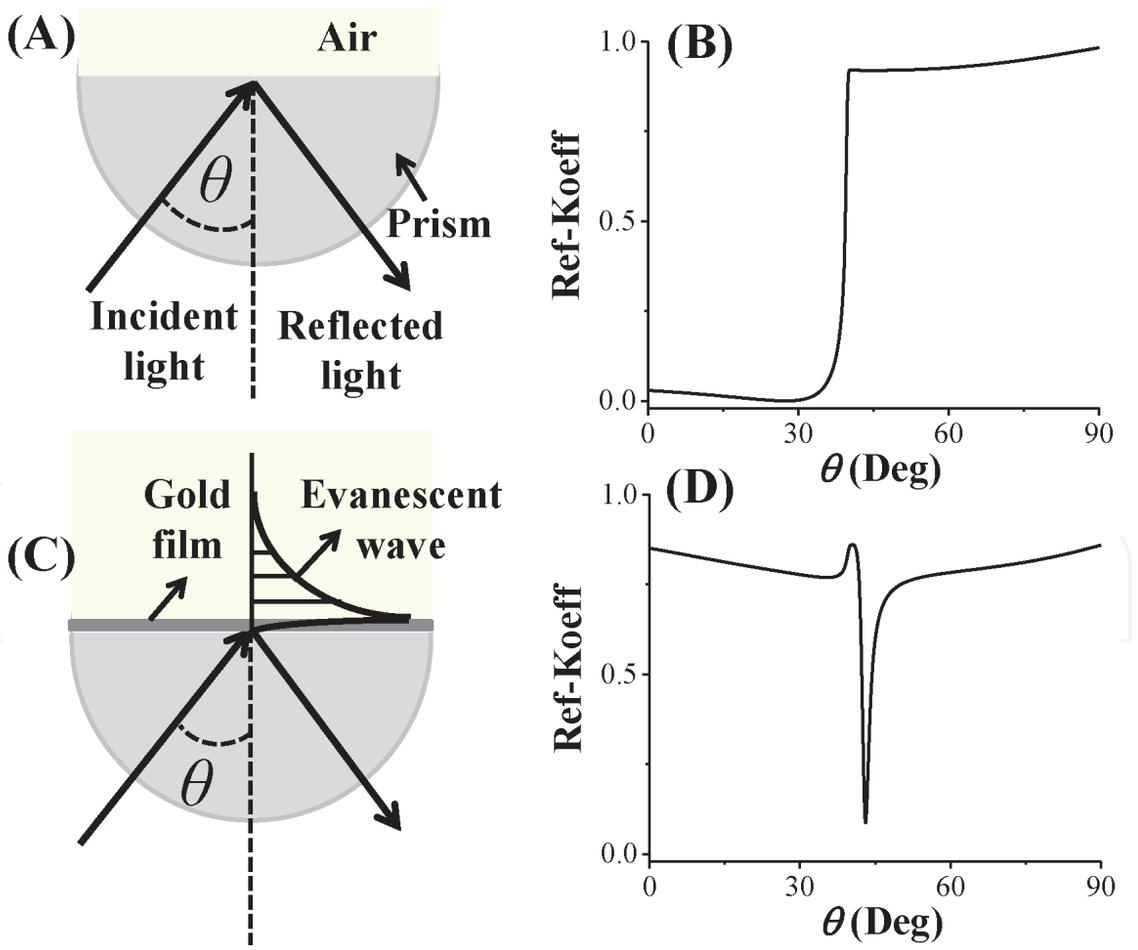

Figure 1.
(A) A polarized light illuminates the interface of air and a prism. (B) The intensity of reflected light corresponding to different incident light angle in panel (A). (C) a polarized light illuminate the interface of gold and prism. The dielectric material on the opposite side of the gold film is air. Panel (D) is the reflected light intensity in panel (C). The dielectric constants of air and the prism are 2.29 and 1, respectively. The thickness of the gold film is 50 nm, and its real and imaginary parts of dielectric constants are −12.3 and 1.29. The simulation was finished via the Winspall software.

As the SP wave intensity decays exponential along with and perpendicular to the propagation direction (**Figure 1C**), the SPR sensor can only be sensitive to the reflective index change next to the metallic surface and the sensitivity decays along with the distance from the metallic surface.

At last, the shape and position (resonance angle) of the dip (**Figure 1D**) are also affected by the reflective index of the materials next to the metallic film. For instance, the dip is much sharper in an air system than water, thus the sensor is more sensitive in an air solution than water.

Similar as Wood's observation, the metallic diffraction grating is also applied to accomplish the SP excitation (**Figure 2**). This method is based on the diffraction of light and is named as grating coupling [16].

The third method is the waveguide coupling method [4]. As is shown in **Figure 3**, a metal film is striped on the wave guiding layer to achieve the SP excitation, and a superstrate is placed on the other side of the metal film for analytic applications.

2.2 Constructions of an SPR sensor

The successful excitations of SP via convenient methods introduce a various applications of this optics. Surface plasmon was first used to characterize thin films in 1978 [2]. In 1982, Nylander and Liedberg applied it to gas detection and biosensors [17].

Nowadays, a series of operation-oriented SPR instruments have been developed. As a result, the main work for the construction of an SPR sensor is choosing an appropriate sensor chip and establishing a reproducible procedure.

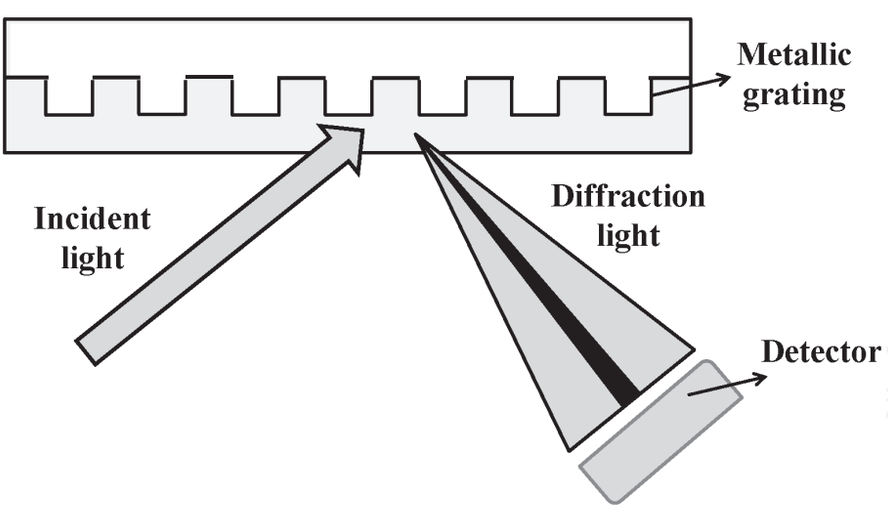

Figure 2.
An incident light with different wavelength illuminate the metallic grating and the narrow dark band is caused by the surface plasmon phenomenon.

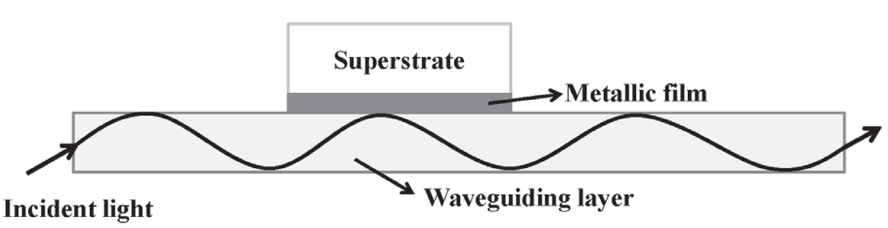

Figure 3.
Waveguide coupling method for surface plasmon excitation.

Nonetheless, a brief introduction on the structure of the SPR sensor is helpful on the construction of an adequate chip. **Figure 4** shows a typical SPR sensor, it consists of the portions for surface plasmon (SP) excitation, solutions delivery, signal detection and conversion, and data processing [18].

The solution delivery portion is applied for the transportation of solutions, which contain the analyte solutions and running buffers. It combines the SP excitation portion on the SPR sensor chip. In a typical Kretschmann geometry, the SP excitation accessories are placed next to the glass side of the sensor chip, and the hydrophobic fluidic channels, which have a width down to hundreds of micrometers, are placed next to the metallic film. The receptors pre-immobilized on the metallic side are reversed for the analytes in the solution transported by the fluidic channels. The reaction between the analytes and receptors causes the reflective index change next to the sensor chip surface (see Section 2.2.3). Furthermore, it causes the resonance angle shift. This shift is online collected by the detector and output as SPR signal. At last, we gather the SPR signal for data processing.

2.2.1 The dilution in the sample delivery

The dilution in the solution delivery process is a hindrance for obtaining reliable data. **Figure 5** shows the concentration distribution of an analyte and its corresponding SPR sensorgram in a system without any molecular reactions or physical adsorptions. This concentration change can be confused with the concentration change caused by the mass transport limitation, and miss leading the data processing procedure.

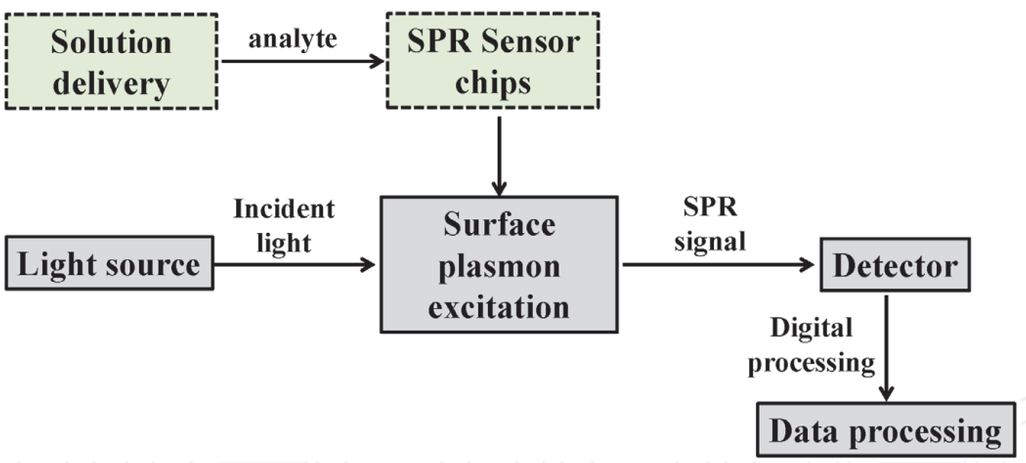

Figure 4.
The configuration of an SPR sensor.

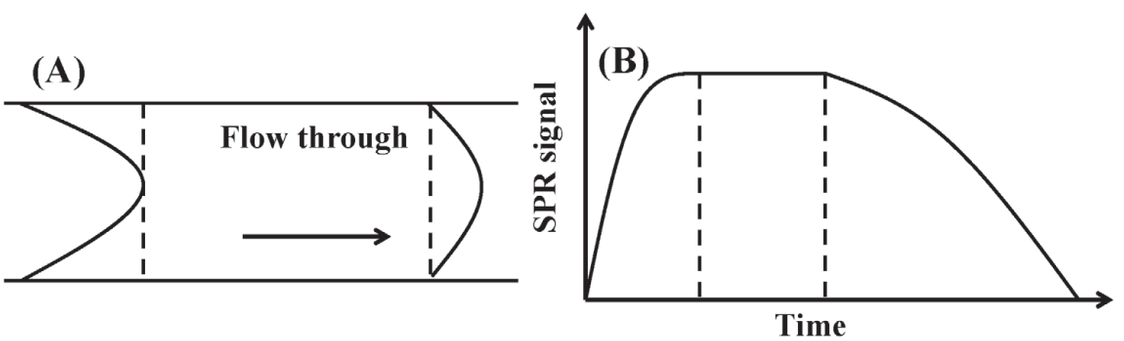

Figure 5.
(A) The dilution in a laminar flow tube during sample delivery. The arrow indicates the flow through direction. (B) The SPR sensorgram of the solution shown in panel (A).

To solve this problem, the microfluidic systems are applied. Also, the bi-direct flow system is efficient on cutting off the diluted samples [19, 20]. In reality, this problem can be alleviated by decreasing the sample delivery distance and increasing the sample delivery rate.

2.2.2 Constructions of SPR sensor chips

SPR sensor chip is the most critical accessory in the whole instrument for the construction of a sensor [21]. It contains a glass substrate and a thin metallic film. For simplify, this glass slide normally has the same reflective index as the prism in the instrument. To simplify the storage condition of the sensor chips and supply a longer shelf life, we usually choose gold film as a substrate. However, silver film supplies a more sensitive experimental condition.

Bare gold chip, containing glass slide and gold film, is the most common used sensor chip and is basic for the constructions of other chips. As this chip is susceptibly contaminated and is not so biocompatible, the surface modifications are essential. Besides, these modifications also satisfy the condition for the receptors immobilization (see Section 2.2.3).

Figure 6 shows the most common applied modification case, the self-assemble method based on the interactions of gold and thiol- or disulfide groups [22]. The uniform of the alkyl chains on the chip surface is maintained by the van der Waals interactive force. The active groups on the other side of the alkyl chains are essential for the immobilization of receptors.

The dextran chip, containing carboxyl groups on the alkyl chain, is applied to construct a series of chips for certain applications. These commercial sensor chips include nitrilotriacetic acid chips (histidine tag capture), streptavidin chips (biotin capture), and lipid capture chips. The chips rely on DNA hybridization or the interactions of streptavidin and biotin are also produced. Other commercial chips contain click chemistry chips, cell capturing chips, and hydrophobic chips [23].

2.2.3 Molecular reactions on the sensor chip

The molecular reactions on the SPR senor chip are different from the reactions in solutions. As is shown in **Figure 7**, receptors (*B*) are immobilized on the sensor chip surface and analytes (*A*) are transported to the fluidic channel on the top of the sensor chip to accomplish the reactions. The immobilization of *A* causes the change

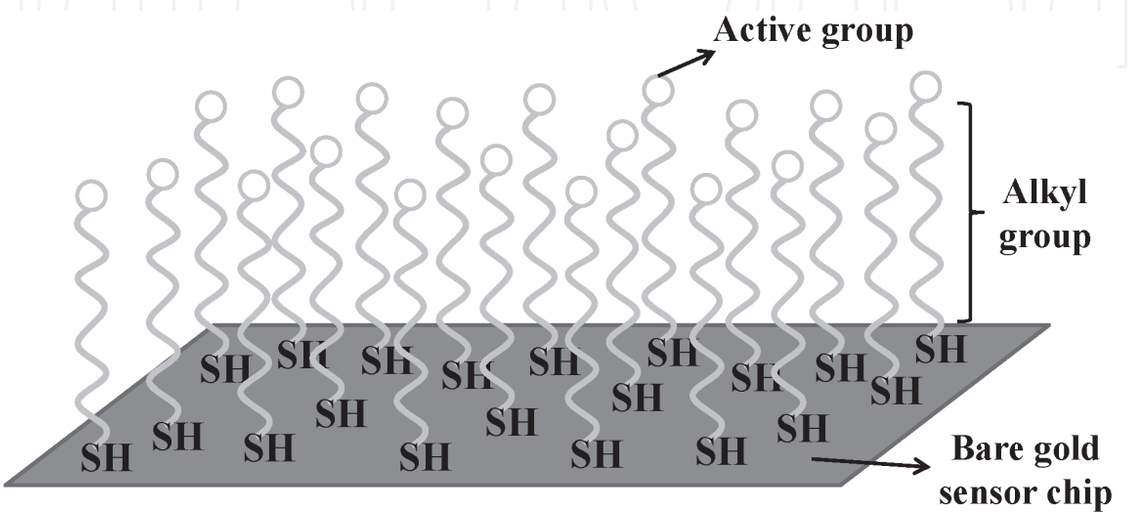

Figure 6.
The self-assembled monolayer on a bare gold sensor chip.

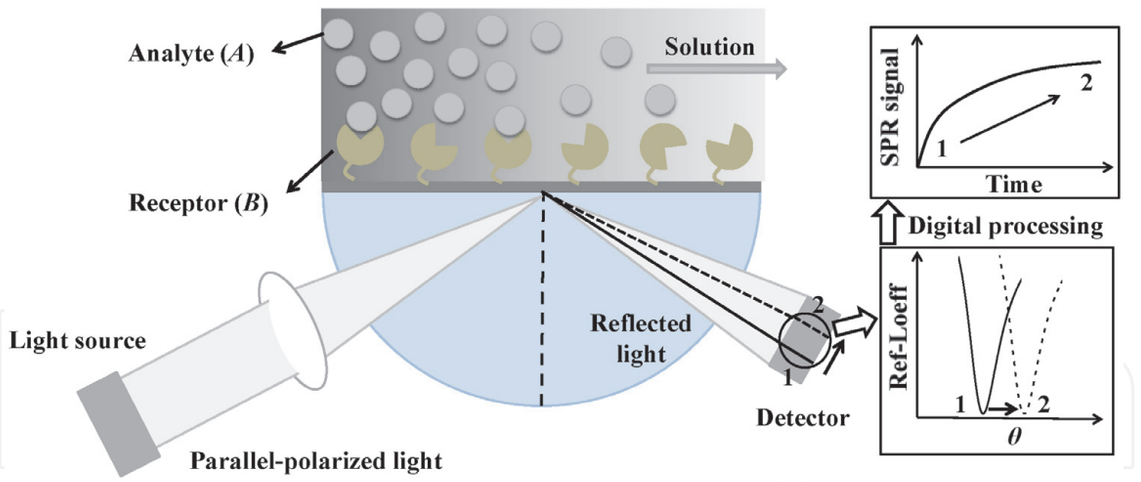

Figure 7.
A scheme shows the bimolecular reactions on the SPR sensor chip surface and the signal transformation in this process.

of reflective index next to the sensor chip surface and further leads to the dip shifting from position 1 to 2 (bottom right in **Figure 7**). This change is recorded by a camera (the detector) and transfers to the SPR signal [24]. By gathering the signal collected at a specific time interval, we obtained the SPR sensorgram and applied it for data processing.

3. Bimolecular interactions

The molecular reactions in reality solutions can be affected by a series of factors, like temperature, concentration, mass transport, and so on. To obtain a better signal, the temperature is normally remained at 25°C in the SPR system. But the temperature control usually allows a higher temperature interval to satisfy different reactions.

As the receptors (B) are pre-immobilized on the chip surface, whose total amount is inalterable, the molecular reaction is the receptors' consumption process. For the analytes (A), they are being transporting to react with B during the binding process. In an ideal condition, the analyte concentration can be maintained the same during the binding process. For the bimolecular reaction between B and A, it can be regard as a pseudo first-order reaction under this circumstance. It is the most common reaction in the SPR system and is a basic reaction for multiple molecules reactions (one B and more than one A).

3.1 Pseudo first-order reaction

Eq. (1) is the bimolecular reaction between B and A in the SPR system at an ideal condition.

$$B + A \underset{k_d}{\overset{k_a}{\rightleftharpoons}} AB \tag{1}$$

where k_a and k_d are the association and dissociation rate constants.

If the binding rate of A is higher than its unbinding rate, the SPR signal increases. In reverse, the signal decreases. **Figure 8** are the SPR sensorgrams showing analytes (A) pass through the fluidic channel in the presence and absence of

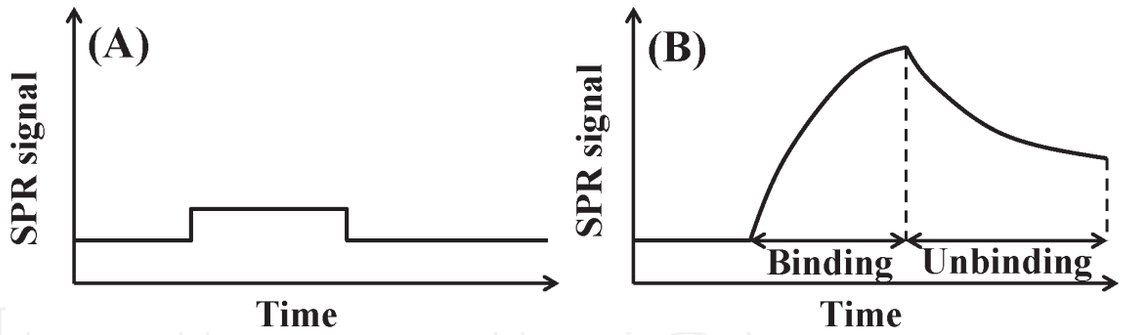

Figure 8.
SPR sensorgram showing analyte A *flow through an SPR sensor chip surface in the absence (A) and presence of* B *(B). On the sensor chip surface,* A *can only react with* B.

receptors (B) on the sensor chip surface. **Figure 8A** shows the concentration change of A without any reactions, and **Figure 8B** is the binding and unbinding of A on the sensor chip surface. By combining the sensorgram with a mathematical approximate model, we obtain the kinetic constants of the reaction.

In an ideal condition, the concentration of analytes, $[A]$ or C, maintains the same during the reaction. The pre-immobilized receptors can be divided into two portions, free receptors on the sensor chip surface (B) and receptors have already been combined with analytes (AB). The formation rate of AB can be expressed as [25, 26].

$$\frac{d[AB]}{dt} = k_a[A][B] - k_d[AB] \tag{2}$$

where $[B]$ is the concentration of free receptors and $[AB]$ is the concentration of AB. As $[AB]$ is proportional to the SPR signal R and the total amount of B is proportional to the highest SPR signal $R_{\max}$, Eq. (2) can be further expressed as

$$\frac{dR}{dt} = k_a C(R_{max} - R) - k_d R \tag{3}$$

After the integral, Eq. (3) can be expressed as

$$R = \frac{k_a C R_{max}}{k_a C + k_d}\left[1 - e^{-(k_a C + k_d)t}\right] \tag{4}$$

At the end of the binding process, $[A]$ or C becomes to zero. Analytes begins to unbind from the sensor chip surface. Eq. (2) can be expressed as

$$\frac{d[AB]}{dt} = -k_d[AB] \tag{5}$$

or

$$\frac{dR}{dt} = -k_d R \tag{6}$$

After the integral, Eq. (6) can be expressed as

$$R = R_0 e^{-k_d t} \tag{7}$$

where R_0 is the SPR signal at the point $[A]$ becomes to zero.

By making a good match between the experimental and simulated sensorgrams, the reaction rate constant k_a and k_d can be obtained. Furthermore, the association and dissociation constants can be obtained via Eq. (8).

$$K_A = \frac{1}{K_D} = \frac{k_a}{k_d} \tag{8}$$

where K_A is the association constant and K_D is the dissociation constant.

At the condition, Eq. (4) is used for concentration detections, a higher amount of receptors have to be pre-immobilized to obtain a higher SPR signal. It also leads to a huge consumption of the analytes. At the point that the amount of analytes bound with receptors is higher than the analytes transported to the sensor chip surface, the concentration of the analyte next to the sensor chip surface changed.

By combining Eqs. (4) and (8), we obtain Eq. (9)

$$R = \frac{R_{max}}{1 + \frac{K}{C}} \left[1 - e^{-(k_a C + k_d)}\right] \tag{9}$$

where R_{max} and K_D are constant for a given reaction. This decreased analyte concentration (C) directly leads to the numerical increase of k_a. But the value of k_a should be the same for a given reaction at a certain temperature and pressure. Thus, the equations above cannot fit any more.

By introducing the mass transport coefficient into the reactions at a mass transfer limited condition [27], we obtain Eq. 10.

$$\mathrm{A} \underset{k_m}{\overset{k_m}{\rightleftarrows}} \mathrm{A} + \mathrm{B} \underset{k_d}{\overset{k_a}{\rightleftarrows}} AB \tag{10}$$

where k_m is the mass transport coefficient. For the laminar flow system in the SPR fluidic channel, k_m can be expressed as

$$k_m = 0.98(D/h)^{2/3}(f/bx)^{1/3} \tag{11}$$

where D is the diffusion coefficient, h and b are the height and width of fluidic channel, f is the volumetric flow rate, x is the distance from the receptor immobilization site.

Still, Eqs. (4) and (7) can be expressed as the following at the mass transport limited condition.

$$R = \frac{k'_a C R_{max}}{k'_a C + k'_d} \left[1 - e^{-\left(k'_a C + k'_d\right)t}\right] \tag{12}$$

and

$$R = R_0 e^{-k'_d t} \tag{13}$$

where k'_a and k'_d are the association and dissociation rate constants at the mass transport limited condition and they can be expressed as

$$k'_a = \frac{k_a k_m}{k_a[B] + k_m} \tag{14}$$

and

$$k'_d = \frac{k_d k_m}{k_a[B] + k_m} \tag{15}$$

Although the association and dissociation rate constants are affected by the mass transport, K_A and K_D can still be calculated via k'_a and k'_d.

$$K_A = \frac{1}{K_D} = \frac{k_d}{k_a} \tag{16}$$

Eq. (12) can be used for concentration detections at mass transport limited condition. Two methods are available, one is built on the equilibrium value R_{eq} and the other one is based on the curve at the beginning of the binding.

R_{eq} is a thermodynamic constant, and it cannot be affected by the mass transport limitation.

$$R_{eq} = \frac{k_a C R_{max}}{k_a C + k_d} = \frac{k'_a C R_{max}}{k'_a C + k'_d} = \frac{C R_{max}}{C + K_D} \tag{17}$$

or

$$\frac{1}{R_{eq}} = \frac{K_D}{R_{max}} \bullet \frac{1}{C} + \frac{1}{R_{max}} \tag{18}$$

Figure 9 are the SPR sensorgrams showing the bimolecular reactions at an ideal (solid line) and a mass transport limited (long dash line) condition. The mass transport limitation significantly prolongs the time to reach the equilibrium. As a result, the method based on R_{eq} is reliable, but not time consuming.

The method based on the curve at the beginning of the binding is attractive, as it is calibration free and high efficient. Although the calibration curve seems to be

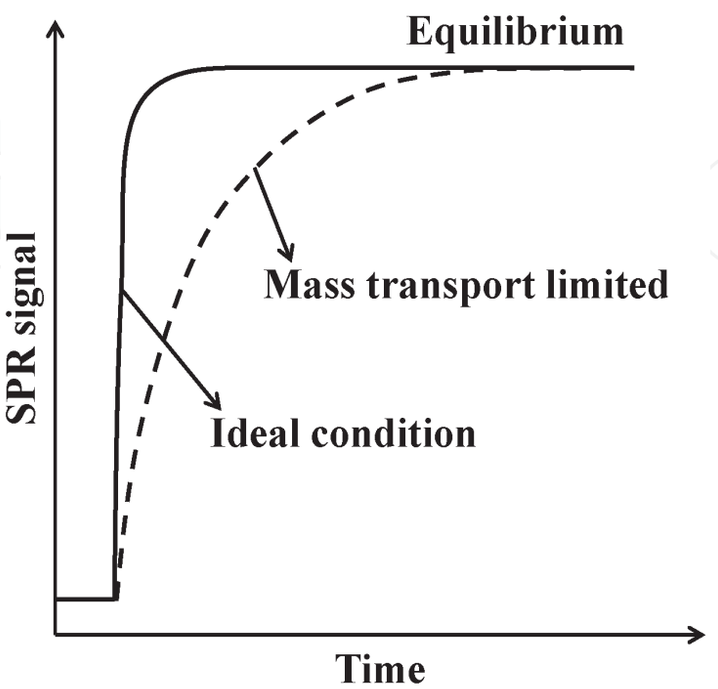

Figure 9.
SPR sensorgrams showing analytes binds to the receptors on the sensor chip surface at the condition with (solid line) and without (long dashed line) mass transport limitation.

ubiquitous and reliable for most of the concentration calculations, the standard samples normally cannot be obtained for a novel biomarker. This significantly hinders the development of the corresponding detection methods.

At a total mass transport limited condition, the binding rate of analytes is decided by the mass transport rate.

$$\frac{dR}{dt} = k_m(C_0 - C) \bullet M_W \bullet 10^9 \tag{19}$$

where C_0 is the analyte concentration in the bulk solution, and M_W is the molecular weight of the analyte. At the beginning of the binding process, C is zero. Thus, this equation can be expressed as

$$\frac{dR}{dt} = k_m C_0 \bullet M_W \bullet 10^9 \tag{20}$$

where the value of dR/dt approximately is equal to the slope of the curve at the beginning of the bimolecular interaction.

3.2 Other reactions

Bimolecular reaction is the basic reaction in some multistep reaction. For instance, the Eq. (21) can be expressed as Eq. (22), which contains two bimolecular reactions.

$$2A + B \underset{k_d}{\overset{k_a}{\rightleftarrows}} A_2B \tag{21}$$

$$A + B \underset{k_{d1}}{\overset{k_{a1}}{\rightleftarrows}} AB + A \underset{k_{d2}}{\overset{k_{a2}}{\rightleftarrows}} A_2B \tag{22}$$

4. Applications

The SPR sensors are available for both concentration and reaction kinetic detections [28]. Their application fields include biological and chemical analyses, drug screening, environmental and food safety monitoring [29].

The concentrations of the biomarkers are essential information for the early diagnose of disease [30]. The reaction kinetics is a crucial parameter for drug screening [31], biological molecules interactions, and chemical industry. The association/dissociation constant is helpful on estimating the strength of the bond [32, 33]. The SPR sensor equipped with different chips affords a friendly condition for the biological molecular reactions. And the chips modified with specific materials (fibronectin, polylysine, and so on) can satisfy the condition for cell culturing [34]. This enlarges the applications of the SPR sensors on biomarker concentration detections, reaction kinetics of molecules, and reaction kinetics between cell membrane and molecules [8].

Natural compounds are usually more biocompatible than synthetic ones, thus they are more suitable drug candidates. But natural compound normally has a low concentration and mixes with other chemicals. The low detection limit and the convenient kinetic detection method make SPR sensors to be widely used in small molecule drug screenings [35]. Furthermore, the high throughput [36, 37] and

mapping technique allow a quick grasp of drugs from natural compounds [22, 23], and even reprocessing of approved drugs.

The contaminants in the environment and food are harmful to our healthy [38, 39]. The SPR sensors not only can detect the concentration of a certain contaminant, but also can make a rough screening of the unknown chemical and biological contaminants. For possible contaminants, the SPR sensor can grasp the molecules or cells for further analyses.

5. Summary

The binding and unbinding of analytes on the SPR sensor chip surface induces the refractive index change next to the thin metallic film. Surface plasmon resonance sensors are sensitive to this refractive index change and transfer this change to the shift of the resonance angle. By a real time recording of the angle change, we obtained the SPR signal for data processing.

The bimolecular reaction is a basic reaction on the sensor chip. By making a good match of the simulated and experimental SPR sensorgrams, we obtained the kinetic constants. Furthermore, we also use the SPR sensors on concentration detections. The concentration detection method based on the R_{eq} value is sensitive but time consuming. The novel calibration free method based on the curve at the beginning of the binding process is time saving. Besides, it efficiently avoids the demand of standard samples. Although its sensitivity is not high, it is still a promising method.

Right now, SPR sensors have been applied in the field of biological and chemical analyses, drug screening, environmental and food safety monitoring. As its integration with new technologies, the application fields of SPR sensors will be further enlarged.

Acknowledgements

Xiaoying Wang participated in the manuscript writing.

Conflict of interest

The authors declare no conflict of interest.

Author details

Xiaoying Wang[1*], Mingqiang Ma[2], Xueliang Wang[3] and Shoujuan Wang[1*]

1 State Key Laboratory of Biobased Material and Green Papermaking, Qilu University of Technology, Jinan, Shandong, China

2 Huadian Electric Power Research Institute Co., Ltd., Hangzhou, Zhejiang, China

3 College of Chemistry and Chemical Engineering, Heze University, Heze, Shandong, China

*Address all correspondence to: xiaoyingw@outlook.com and nancy5921@163.com

References

[1] Wood RWXLII. On a remarkable case of uneven distribution of light in a diffraction grating spectrum. Philosophical Magazine. 1902;**4**: 396-402. DOI: 10.1080/14786440209462857

[2] Pockrand I, Swalen JD, Gordon JG, Philpott MR. Surface plasmon spectroscopy of organic monolayer assemblies. Surface Science. 1978;**74**: 237-244. DOI: 10.1016/0039-6028(78)90283-2

[3] Gordon JG, Ernst S. Surface plasmons as a probe of the electrochemical interface. Surface Science. 1980;**101**:499-506. DOI: 10.1016/0039-6028(80)90644-5

[4] Homola J. Electromagnetic theory of surface plasmons. In: Homola J, editor. Surface Plasmon Resonance Based Sensors. Berlin, Heidelberg: Springer; 2006. pp. 3-44

[5] Stojanović I, Schasfoort RBM, Terstappen LWMM. Analysis of cell surface antigens by surface plasmon resonance imaging. Biosensors & Bioelectronics. 2014;**52**:36-43. DOI: 10.1016/j.bios.2013.08.027

[6] Kurinomaru T, Kojima N, Kurita R. Sequential assessment of multiple epigenetic modifications of cytosine in whole genomic DNA by surface plasmon resonance. Analytical Chemistry. 2019;**91**:13933-13939. DOI: 10.1021/acs.analchem.9b03423

[7] Peng T, Li X, Li K, Nie Z, Tan W. DNA-modulated plasmon resonance: Methods and optical applications. ACS Applied Materials & Interfaces. 2020;**12**:14741-14760. DOI: 10.1021/acsami.9b23608

[8] Bocková M, Slabý J, Špringer T, Homola J. Advances in surface plasmon resonance imaging and microscopy and their biological applications. Annual Review of Analytical Chemistry. 2019; **12**:151-176. DOI: 10.1146/annurev-anchem-061318-115106

[9] Yang HM, Teoh JY, Yim GH, Park Y, Kim YG, Kim J, et al. Label-free analysis of multivalent protein binding using bioresponsive nanogels and surface plasmon resonance (SPR). ACS Applied Materials & Interfaces. 2020;**12**: 5413-5419. DOI: 10.1021/acsami.9b17328

[10] Stojanović I, Ruivo CF, van der Velden TJG, Schasfoort RBM, Terstappen LWMM. Multiplex label free characterization of cancer cell lines using surface plasmon resonance imaging. Biosensors. 2019;**9**:70. DOI: 10.3390/bios9020070

[11] Štěpánek J, Vaisocherová H, Piliarik M. Molecular interactions in SPR sensors. In: Homola J, editor. Surface Plasmon Resonance Based Sensors. Berlin, Heidelberg: Springer; 2006. pp. 69-91

[12] Fano U. The theory of anomalous diffraction gratings and of quasi-stationary waves on metallic surfaces (Sommerfeld's waves). Journal of the Optical Society of America. 1941;**31**:213-222. DOI: 10.1364/JOSA.31.000213

[13] Homola J, Piliarik M. Surface plasmon resonance (SPR) sensors. In: Homola J, editor. Surface Plasmon Resonance Based Sensors. Berlin, Heidelberg: Springer; 2006. pp. 45-67

[14] Kretschmann E, Raether H. Notizen: Radiative decay of non radiative surface plasmons excited by light. Zeitschrift für Naturforschung A. 1968;**23**:2135-2136. DOI: 10.1515/zna-1968-1247

[15] Otto A. Excitation of nonradiative surface plasma waves in silver by the method of frustrated total reflection.

Zeitschrift für Physik. 1968;**216**: 398-410. DOI: 10.1007/BF01391532

[16] Ruemmele JA, Hall WP, Ruvuna LK, Van Duyne RP. A localized surface plasmon resonance imaging instrument for multiplexed biosensing. Analytical Chemistry. 2013;**85**:4560-4566. DOI: 10.1021/ac400192f

[17] Nylander C, Liedberg B, Lind T. Gas detection by means of surface plasmon resonance. Sensors and Actuators. 1982; **3**:79-88. DOI: 10.1016/0039-6028(80) 90644-5

[18] Nguyen HH, Park J, Kang S, Kim M. Surface plasmon resonance: A versatile technique for biosensor applications. Sensors (Basel). 2015;**15**:10481-10510. DOI: 10.3390/s150510481

[19] Wang S, Boussaad S, Tao N. Surface plasmon resonance spectroscopy: Applications in protein adsorption electrochemistry. In: Rusling JF, editor. Biomolecular Films: Design, Function, and Applications. New York: Marcel Dekker; 2003. pp. 213-251

[20] Wang X, Zhou F. Dual-valve and counter-flow surface plasmon resonance. Analytical Chemistry. 2018; **90**:4972-4977. DOI: 10.1021/acs. analchem.8b00277

[21] Masson J-F, Battaglia TM, Cramer J, Beaudoin S, Sierks M, Booksh KS. Reduction of nonspecific protein binding on surface plasmon resonance biosensors. Analytical and Bioanalytical Chemistry. 2006;**386**:1951-1959. DOI: 10.1007/s00216-006-0834-2

[22] Mrksich M, Sigal GB, Whitesides GM. Surface plasmon resonance permits in situ measurement of protein adsorption on self-assembled monolayers of alkanethiolates on gold. Langmuir. 1995;**11**:4383-4385. DOI: 10.1021/la00011a034

[23] Gedig ET. Surface chemistry in SPR technology. In: Richard BMS, editor. Handbook of Surface Plasmon Resonance (2). Cambridge, UK: The Royal Society of Chemistry; 2017. pp. 171-254

[24] Hinman SS, McKeating KS, Cheng Q. Surface plasmon resonance: Material and interface design for universal accessibility. Analytical Chemistry. 2018;**90**:19-39. DOI: 10.1021/acs.analchem.7b04251

[25] Karlsson R, Roos H, Fägerstam L, Persson B. Kinetic and concentration analysis using BIA technology. Methods. 1994;**6**:99-110. DOI: 10.1006/ meth.1994.1013

[26] Zhao H, Schuck P. Detailed analysis of kinetic binding traces with distributions of surface sites. In: Richard BMS, editor. Handbook of Surface Plasmon Resonance. Cambridge, UK: The Royal Society of Chemistry; 2017. pp. 149-170

[27] Pol E, Roos H, Markey F, Elwinger F, Shaw A, Karlsson R. Evaluation of calibration-free concentration analysis provided by biacore systems. Analytical Biochemistry. 2016;**510**:88-97. DOI: 10.1016/j.ab.2016.07.009

[28] Singh P. SPR biosensors: Historical perspectives and current challenges. Sensors and Actuators B: Chemical. 2016;**229**:110-130. DOI: 10.1016/j. snb.2016.01.118

[29] Rich RL, Myszka DG. Survey of the 2009 commercial optical biosensor literature. Journal of Molecular Recognition. 2011;**24**:892-914. DOI: 10.1002/jmr.1138

[30] Choi J-H, Lee J-H, Son J, Choi J-W. Noble metal-assisted surface plasmon resonance immunosensors. Sensors. 2020;**20**:1003. DOI: 10.3390/s20041003

[31] Nunes NM, de Paula HMC, Coelho YL, da Silva LHM, Pires ACS.

Surface plasmon resonance study of interaction between lactoferrin and naringin. Food Chemistry. 2019;**297**: 125022. DOI: 10.1016/j.foodchem.2019.125022

[32] Pelosi P, Zhu J, Knoll W. From radioactive ligands to biosensors: Binding methods with olfactory proteins. Applied Microbiology and Biotechnology. 2018;**102**:8213-8227. DOI: 10.1007/s00253-018-9253-5

[33] Juhász Á, Luty-Błocho M, Wojnicki M, Tóth GK, Csapó E. General method for kinetic and thermodynamic evaluation of a receptor model peptide-drug molecule interaction studied by surface plasmon resonance. Microchemical Journal. 2019;**147**: 311-318. DOI: 10.1016/j.microc.2019.03.048

[34] Kreysing E, Seyock S, Hassani H, Brauweiler-Reuters E, Neumann E, Offenhäusser A. Surface plasmon resonance microscopy: Correlating surface plasmon resonance microscopy of living and fixated cells with electron microscopy allows for investigation of potential preparation artifacts. Advanced Materials Interfaces. 2020;**7**: 2070026. DOI: 10.1002/admi.202070026

[35] Honarmand S, Dabirmanesh B, Amanlou M, Khajeh K. The interaction of several herbal extracts with α-synuclein: Fibril formation and surface plasmon resonance analysis. PLoS One. 2019;**14**:e0217801. DOI: 10.1371/journal.pone.0217801

[36] Wegner GJ, Wark AW, Lee HJ, Codner E, Saeki T, Fang S, et al. Real-time surface plasmon resonance imaging measurements for the multiplexed determination of protein adsorption/desorption kinetics and surface enzymatic reactions on peptide microarrays. Analytical Chemistry. 2004;**76**:5677-5684. DOI: 10.1021/ac0494275

[37] Wang Y, Zhang C, Zhang Y, Fang H, Min C, Zhu S, et al. Investigation of phase SPR biosensor for efficient targeted drug screening with high sensitivity and stability. Sensors and Actuators B: Chemical. 2015;**209**: 313-322. DOI: 10.1016/j.snb.2014.11.134

[38] Homola J. Surface plasmon resonance biosensors for food safety. In: Narayanaswamy R, Wolfbeis OS, editors. Optical Sensors: Industrial Environmental and Diagnostic Applications. Berlin, Heidelberg: Springer; 2004. pp. 145-172

[39] García-Aljaro C, Muñoz-Berbel X, Jenkins ATA, Blanch AR, Muñoz FX. Surface plasmon resonance assay for real-time monitoring of somatic coliphages in wastewaters. Applied and Environmental Microbiology. 2008;**74**: 4054-4058. DOI: 10.1128/aem.02806-07